PCCP

Accepted Manuscript

ROYAL SOCIETY OF CHEMISTRY

www.rsc.org/pccp

Cite this: DOI: 10.1039/c0xx00000x

www.rsc.org/xxxxxx

ARTICLE TYPE

Tinene: A two-dimensional Dirac material with 72 meV band gap

*Bo Cai[1], Shengli Zhang[1], Ziyu Hu[2], Yonghong Hu[1], Yousheng Zou[1], Haibo Zeng[1]**

[1]Institute of Optoelectronics &Nanomaterials, College of Materials Science and Engineering, Nanjing University of Science and Technology, Nanjing 210094, China

[2]Beijing Computational Science Research Center,Beijing 100084, People's Republic of China

*Corresponding Author: zeng.haibo@njust.edu.cn

Received (in XXX, XXX) Xth XXXXXXXXX 20XX, Accepted Xth XXXXXXXXX 20XX
DOI: 10.1039/b000000x

Dirac materials have attracted great interests for both fundamental research and electronic device ("devices" in original version) due to their unique band structures ("structure" in original version), but the usual near zero bandgap of graphene results in a poor ("low" in original version) on-off ratio in the corresponding transistors. Here, we report on tinene, monolayer gray tin, as a new two-dimensional material with both Dirac characteristic and remarkable 72 meV bandgap based on density function theory calculations (insert "calculations"). Compared with silicene and germanene, tinene has similar hexagonal honeycomb monolayer structure, but it is ("is of" in original version) obviously larger buckling height (~ 0.70 Å). Interestingly, such moderate buckling structure (insert "structure") results in phonon dispersion without appreciable imaginary modes, indicating the strong dynamic stability of tinene. Significantly, a distinct transformation is ("was" in original version) discovered form the band structure that six Dirac cones would ("will" in original version) appear at high symmetry K points in the first Brillouin zone when gray tin is thinned from bulk to monolayer, but a bandgap as large as 72 meV is still preserved. Considering the recent successful realizations of silicene and germanene with similar structure, the predicted stable tinene with Dirac characteristic and suitable bandgap is worth highly expecting for the "more than moore" materials and devices.

Graphene, the representative of two-dimensional (2D) materials, appeals to scientific community since it was successfully synthesized through mechanical methods due to its large surface, and unique properties from mechanical to electronic[1-4]. It has been revealed that graphene has six Dirac cones which are formed by the π and π* bands at high symmetric K points; hence (delete "and") graphene has ("have" in original version) excellent electrical properties and special carrier characteristics. Around the Dirac cones, linear dispersion indicates that effective electronic mass is zero and Fermi velocity is closed to speed of light. Zero effective electronic mass and high Fermi velocity determines graphene (Fermi velocities has been corrected to singular form and the word "has" after "graphene" has been deleted) excellent electronic transportation performance. However, the zero bandgap greatly limits on-off ratio in transistor and has no matched light wavelength. So graphene can hardly be used to transistors and optoelectronic devices[5-7], for example, field effect transistor (FET), bipolar junction transistor (BJT), photovoltaic cell, et al.

On the other hand, the discovery of graphene overthrow our misunderstanding that 2D crystal cannot exist stably in real three dimensional world[1, 8]. Nowadays, the synthetic methods of 2D materials have been well established ("mature" in original version), including mechanical cleavage[1], liquid phase and gas phase exfoliation[9], crystal growth extension[10], and oxidation-reduction methods[11]. These methods have even been applied to realize many other 2D materials. Recently, silicene, which is previously predicted as 2D Dirac material, has been successfully grown on Ag substrates[12-15]. As another 2D Dirac material, germanene is also ("also was also" in original version) a kind of stable 2D material in theory through phonon dispersion[12, 16]. Lately, germanene has been successfully fabricated on the substrate Pt (111)[17]. Having a small band gap is the most important difference of silicene and germanene from graphene, which has been expected to remedy the zero-bandgap weakness of graphene. However, these two new kinds of 2D Dirac materials are still very hard to fabricate currently, and they are still hardly used to manufacture devices although great efforts have been paid to tune the bandgap through many ways, including external electric field[18-20], biaxial strain[21], compounds metal[22, 23], surface adsorption[24], oxidation of silicene[25], substrate effect[26], being hydrogenated[27], new phase structure[28]. Therefore, finding stable 2D Dirac materials with moderate bandgap is still in a great challenge, but high expected for the "more than moore" materials and devices.

In this paper, we report on tinene, monolayer gray tin, as a new 2D material to be of moderate buckling degree, high dynamic stability, Dirac electronic characteristic, as well as remarkable 72 meV bandgap. It is found that tinene has similar hexagonal honeycomb monolayer structure to silicene and germanene, but it is (delete "of") obviously large ("larger" in original version) buckling height (~ 0.70 Å), which endows its high dynamic stability, shown by the phonon dispersion without appreciable imaginary modes. Most importantly, a distinct transformation is discovered form the band structure that six Dirac cones appear at high symmetry K points in the first Brillouin zone when gray tin thins from bulk to monoatomic sheet in diamond structure, but a bandgap as large as 72 meV is still preserved. Such co-existence of Dirac characteristic and suitable bandgap makes tinene worth highly expecting for the "more than moore" materials and devices.

Computational details.

All the density functional calculations are performed by using the CASTEP code with a norm-conserving pseudo-potential, under periodic boundary. Geometry optimization and band structure calculations are under the generalized gradient approximation (GGA) of the Perdew, Burke, and Ernzerholf (PBE) form and the Perdew-Wang (PW91) form, the Local Density Approximation (LDA) of the Ceperly−Alder−Perdew−Zunger (CA-PZ). The kinetic energy cutoff of the plane wave is set to 500 eV on a grid of 30×30×1 k-points for the tinene. The geometry of the configuration is optimized by using Broyden-Fletcher-Goldfarb-Shanno (BFGS) minimizer. The self-consistent convergence accuracy is set at 5×10^{-6} eV per atom, the convergence criterion for the force between atoms is 0.01 eV per Å, and the maximum displacement is 5.0×10^{-4} Å. A sufficiently large 20 Å vacuum region is used to separate the two-dimensional structures to rule out any interaction among the neighboring layers along c-axis. Considering that standard GGA functional and LDA functional always underestimate the band gap values, we also employe a more accurate hybird functional proposed by HSE06 in the electronic structure calculations. The kinetic energy cutoff is set to 500 eV on a grid of 5×5×1 k-points. Other parameters are exactly same. Raman spectrum, phonon, and electron energy loss spectroscopy calculation are only performed by using the greneralized-gradient-approximation (GGA) of the Perdew, Burke, and Ernzerholf (PBE) form.

Results

Tinene structures.

Tin, following silicon and germanium in the fourth group of periodic table of elements, has two stable allotropes of white and gray tin under normal atmospheric pressure. 13.2℃ is the critical temperature for the transformation from gray tin (below 13.2℃) to white tin (up 13.2℃). Similar to silicon and germanium, bulk gray tin also has a typical diamond structure with space group of $Fd\bar{3}m$ (No. 227) as shown in Fig. 1(a). After full relaxation, the optimal structure of tinene is presented in Fig. 1 (b-d). From the side view (Fig. 1(b)), tinene has an obviously buckled structure with longitudinal displacement of 0.73 Å, which is larger than those of silicone (Δ=0.45 Å) and germanene (Δ=0.68 Å). From the top view (Fig. 1(c)), tinene is very similar to the hexagonal honeycomb planar lattice of silicene. Each unit cell of tinene contains two atoms (space group $P\bar{3}m1$, No.164). The buckled structure of tinene is consisted of many interlinked ruffled six-membered rings with the diagonal line length of 5.16 Å. In the fully relaxed tinene, each tin atom is connected to three nearest neighbour atoms with bond length of 2.68 Å and bond angle of 112.9° (Fig. 1(d)). The detailed structural parameters of tinene for different methods are given in **Table 1** with comparisons of graphene, silicene and germanene.

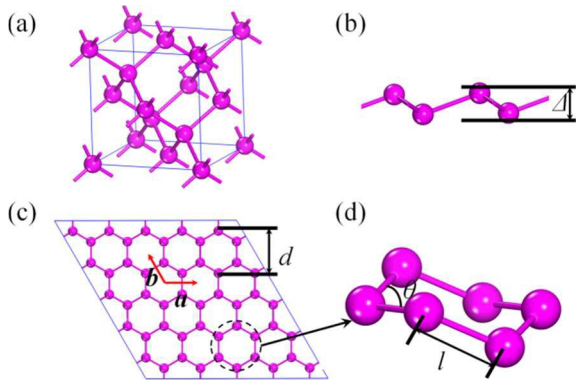

Fig. 1 (a) diamond structure of gray tin. (b) side view, low buckling structure for tinene, germanene and silicene are like this. (c) top view, vector *a* and *b* are basis vector of primitive cells, *d* is the width of hexagonal ring. (d) bond length of Sn-Sn (*l*) and bond angle of Sn-Sn-Sn (θ) are given. For graphene, the buckling height Δ is zero.

	a(Å)	Δ(Å)	*d*(Å)	θ (°)	*l*(Å)
Tinene (LDA)	4.52	0.70	5.21	113.5	2.70
Tinene (PW91)	4.52	0.69	5.22	113.7	2.70
Tinene (PBE)	4.47	0.73	5.16	112.9	2.68
Tinene(HSE06)	4.48	0.70	5.17	113.5	2.68
Germanene	3.97	0.64	4.58	113.0	2.38[29]
	4.02	0.68	4.64	112.4	2.42
Silicene	3.83	0.44	4.41	116.4	2.25[29]
	3.86	0.45	4.45	116.1	2.27
Graphene	2.46	0	2.84	120.0	1.42[29]
	2.47	0	2.85	120.0	1.43

Table1 Structural parameters of tinene, germanene, silicene and graphene, for their most energetically stable atomic configurations.

Phonon dispersion and stability.

For a newly proposed 2D material, its stability is crucial for the future experimental realization. Here, the dynamically stability of tinene is analyzed through phonon dispersion. The calculated phonon dispersion is presented in Fig. 2. Very excitingly, there is no any imaginary frequency in calculated phonon dispersion. Actually, similar results have been previously reported for silicene and germanene to verify their stabilities[12]. Therefore, such consequence reveals that tinene is also dynamically stable. Hence the 2D structure (“such 2D structure” in original version) is possible to be realized in future experiments, for example through epitaxial growth on Pt (111), Ag (111) or Ir (111) substrates. To further verify the crucial contribution of moderate buckling to the outstanding stability, a completely planar monoatomic sheet tinene (***Δ=0***) is constrainedly defined, and the corresponding phonon dispersion is also given in Fig. 2. As expected, obvious imaginary frequency appears in the phonon

dispersion of such monolayer tinene, indicating the impossible existence of the completely planar tinene and the important function of moderate buckling on the stable existence of tinene.

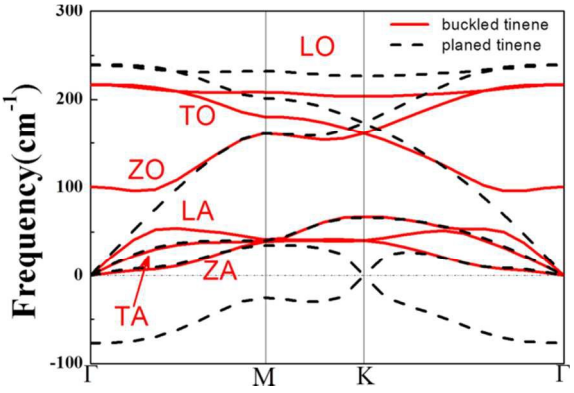

Fig. 2 The phonon dispersion of two different structures of tinene, low buckled (LB) structure (red line) are stable and planed structure (black dashed) are unstable.

Raman spectra reflect vibrational modes of atoms. It is a measure for characteristic materials in experiments and related to phonon dispersion in simulation. Raman spectra are given by Fig. 3. It can be seen that the vibrational frequencies of tinene are relatively lower than these of (insert "these of") silicene and germanene[30, 31]. Such as, the doubly degenerate E_g mode of tinene is found to locate at 217 cm^{-1} (ω_Γ) while silicene and germanene is 562 and 303 cm^{-1}, respectively. This is also well confirmed by the following Raman spectra as shown in Fig. 3(a). In first principle theory, the location of Raman spectrum peaks is corresponding to the value of phonon dispersion at high symmetric point Γ. Optic vibrational mode is relative movement of each atom in unit cells, while centre of unit cells are static (Fig. 3(a)). On the contrary, acoustic vibrational mode is vibrational of unit cells, while all atoms in unit cells stay relative movements (Fig. 3(b)). It is found that an intense peak at about 217 cm^{-1} and another lower one at about 100 cm^{-1} are exhibited in the calculated Raman spectra. From the analysis of the vibrational mode, we can understand that the peak at about 217 cm^{-1} is attributed to the in-plane transverse optic branch (TO) and the in-plane longitudinal optic branch (LO) vibrational modes, and the peak at about 100 cm^{-1} is attributed to the out-of-plane transverse optic branch (ZO) mode. Actually, the TO Raman mode of tinene could be considered as the counterpart of the G peak in graphene at 1600 cm^{-1} [30]. Why vibrational frequencies of tinene are lower than graphene, silicene and germanene? As we know, heavy atoms vibrate more difficult than light atoms. Tin atom is heavier than carbon, silicon and germanium atom. This can explain this phenomenon well. Hence it can be used as a fingerprint to confirm the formation of monolayer tinene in the future experiments.

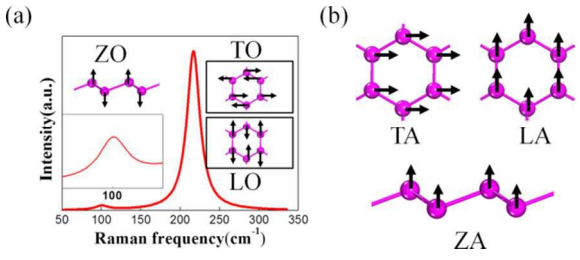

Fig. 3 (a) Raman spectra and the peaks corresponding optic branch vibrational mode of tinene. (b) acoustic branch vibrational mode of tinene which not corresponding peaks in Raman spectrum.

Electronic Properties.

Dirac material has interesting physics performance, such as its charge carriers can be regarded as massless Dirac fermions and it has spectacular physics phenomena quantum Hall effects. One way to distinguish Dirac materials is band structure. Band structures of bulk gray tin and monolayer tinene are shown in Fig. 4. Band structures of bulk gray tin along the highly symmetric L-Γ-X path in Brillouin zone are given by Fig. 4(a). Conduction band minimum (CBM) and valence band maximum (VBM) have no discontinuous point and tangent to each other at Γ point. This means that bulk gray tin exhibits the typical semimetal behaviour, not a Dirac material. While VBM and CBM of tinene, germanene and silicene along the highly symmetric Γ-M-K-Γ directions in Brillouin zone take a linear distribution around Fermi level E_F at high symmetric point $\boldsymbol{q}$=K with GGA-PBE methods, given by Fig. 4(b). The linear dispersion indicates that massive electron quasiparticles are called massless Dirac fermions, which can be seen as electrons that lost their rest mass m_0. Another feature of Dirac fermions is that these quasiparticles described by Dirac equation with an effective speed of light. According to linear spectrum $E=\hbar v_F \boldsymbol{k}$, $\boldsymbol{k}$ is quasiparticle momentum, Fermi velocity v_F of graphene is 0.99×10^6 m/s and for tinene is 0.72×10^6 m/s in our work. Besides lower Fermi velocity compared to graphene, having a small gap of 72 meV with HSE06 methods is the most clearly differentiates from graphene.

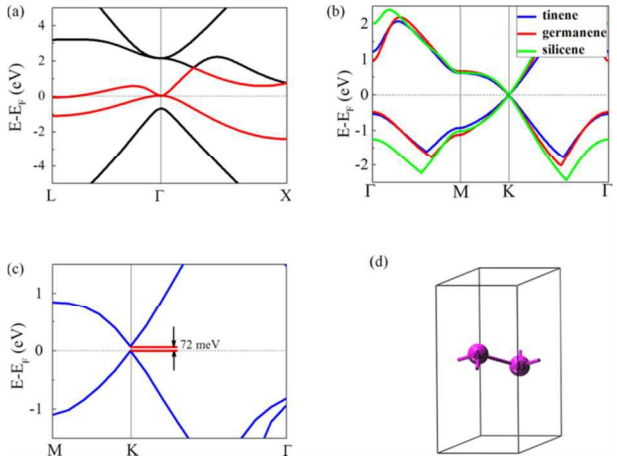

Fig. 4 (a) band structures of bulk gray tin, red lines are CBM and VBM. (b) CBM and VBM of silicene (green line), germanene (red line) and tinene (blue line) with GGA-PBE method. (c) Dirac cones with 72 meV for tinene with HSE06 method. (d) two sublattices A and B in one unit cell.

As we know, Dirac points in a hexagonal graphene are due to the presence of two sublattices. In tinene, each tin atom connects three other tin atoms through σ bond, and with the σ bond length increased, the strength of σ bond decreased. In graphene, the σ bond is strong enough to keep all carbon atoms in a plane, while in tinene the σ bond is not stronger enough. Thus, graphene is consisted of two equivalent sublattices, but each tin atom on a honeycomb lattice with one sublattice slightly shifted out of the plane of the other sublattice (as shown in Fig.4(d)). In this case, a different tight-binding (TB) model needs to be derived. Tinene is closely related to the structure of a monoatomic sheet of diamond gray tin (1 1 1) and this should allow we to derive a TB Hamiltonian closely related to bulk gray tin Hamiltonian that

reduces to the planed structure. As a consequence, the π and σ electrons are automatic coupling and Dirac points features are preserved for LB structure. On the other hand, coupling of Dirac fermions to an Einstein phonon modeled with a Holstein Hamiltonian can lead to modify the gap.[32] This may be the origin of the small gap of tinene.

Optical properties.

To provide a characterization of tinene we provide the optical properties of tinene. Electron energy loss spectroscopy is a powerful technique to probe the dielectric function of material and it is used to distinguish few-layer coating silicene and germanene[33, 34]. It's not difficult to prove that numbers of electrons without occurring inelastic scattering exponential decay along with the sample thickness.

Here, we get the dielectric function of tinene (Fig. 5(a) and (b)). And we provide a way to recognized tinene through energy loss function (Fig. 5). We give two directions EELS (Fig. 5(c) for out-of-plane-polarization and Fig. 5(d) for in-plane polarization). The out-of-plane-polarization spectra (E||c) have only π+σ plasmon peaks (about 6.99 eV). While the in-plane-polarization spectra (E⊥c) have two sections, including π plasmon peaks (below 5 eV) and π+σ plasmon peaks (above 5 eV). The π plasmon feature arises due to the collective π–π* transitions, while the π*+σ plasmon results from the π-σ* and σ-σ excitations.

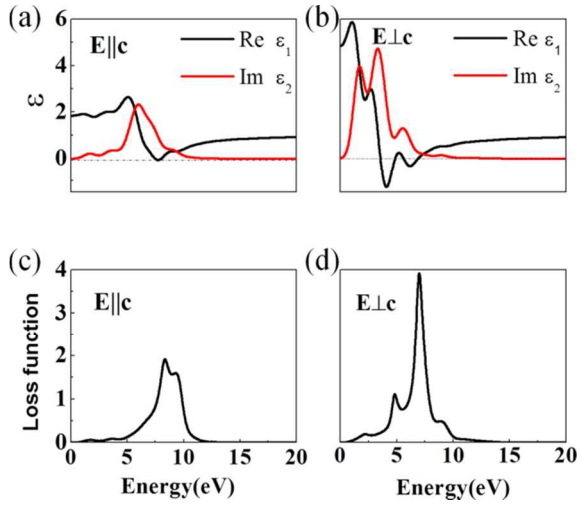

Fig. 5 (a) real and imaginary part of dielectric function of tinene for out-of-plane polarization (E||c). (b) real and imaginary part of dielectric function of tinene for in-plane polarization (E⊥c). (c) electron energy loss function of tinene for out-of-plane polarization (E||c). (d) electron energy loss function of tinene for in-plane polarization (E⊥c).

Conclusions

In summary, we predict a new two-dimensional Dirac material tinene by first principle DFT calculations. Tinene has a buckling two-dimensional structure similar to silicene and germanene, but buckling height is larger than silicene and germanene. The bond characteristics of tinene are closer to the sp^3 hybridization than sp^2 hybridization, although each tin atom has only three covalent bonds. This structure is stable through phonon dispersion study. Tinene (delete "monolayer") has three vibrational modes (LO, TO and ZO) at high symmetric Γ point. It has a Dirac point which is found at high symmetric point K in first Brillouin zone, similar to graphene. It shows that electronic mass is zero and Fermi velocity is nearly light speed. The EELS shows that out-of-plane polarization spectrum (E||c) only has the peak of π+σ plasmon peak at about 6.99 eV and in-plane polarization spectrum (E⊥c) has two sections including π plasmon peaks (below 5 eV) and π+σ plasmon peaks (above 5 eV). Our study of tinene may provide a new material that has possibility to be applied in microelectronic devices.

Acknowledgements

This work was financially supported by the National Basic Research Program of China (2014CB931700), NSFC (61222403, 11274173), the Doctoral Program Foundation of China (20123218110030), the Opened Fund of the State Key Laboratory on Integrated Optoelectronics (IOSKL2012KF06), Natural Science Foundation of Jiangsu province (No. BK20140769).

Author contributions

B. C., S. L. Z.; Z. Y. H. performed the calculations; Y. H. H., Y. S. Z. and H. B. Z. prepared the manuscript. All authors reviewed the manuscript.

Notes and references

1. K. S. Novoselov, A. K. Geim, S. V. Morozov, D. Jiang, Y. Zhang, S. V. Dubonos, I. V. Grigorieva and A. A. Firsov, *Science*, 2004, 306, 666-669.
2. K. S. Novoselov, A. K. Geim, S. V. Morozov, D. Jiang, M. I. Katsnelson, I. V. Grigorieva, S. V. Dubonos and A. A. Firsov, *Nature*, 2005, 438, 197-200.
3. A. H. Castro Neto, F. Guinea, N. M. R. Peres, K. S. Novoselov and A. K. Geim, *Rev. Mod. Phys.*, 2009, 81, 109-162.
4. A. K. Geim and K. S. Novoselov, *Nat. Mater.*, 2007, 6, 183-191.
5. B. Huang, H.-X. Deng, H. Lee, M. Yoon, B. G. Sumpter, F. Liu, S. C. Smith and S.-H. Wei, *Phys. Rev. X*, 2014, 4, 021029.
6. V. Q. Bui, T.-T. Pham, H.-V. S. Nguyen and H. M. Le, *J. Phys. Chem. C*, 2013, 117, 23364-23371.
7. A. I. Shkrebtii, E. Heritage, P. McNelles, J. L. Cabellos and B. S. Mendoza, *Phys. Status Solidi C*, 2012, 9, 1378-1383.
8. N. D. Mermin, *Phys. Rev.*, 1968, 176, 250-254.
9. X. Li, G. Zhang, X. Bai, X. Sun, X. Wang, E. Wang and H. Dai, *Nat. Nanotechnol.*, 2008, 3, 538-542.
10. P. W. Sutter, J.-I. Flege and E. A. Sutter, *Nat. Mater.*, 2008, 7, 406-411.
11. S. Park and R. S. Ruoff, *Nat. Nanotechnol.*, 2009, 4, 217-224.
12. Y. Cai, C.-P. Chuu, C. M. Wei and M. Y. Chou, *Phys. Rev. B*, 2013, 88, 245408.
13. A. Resta, T. Leoni, C. Barth, A. Ranguis, C. Becker, T. Bruhn, P. Vogt and G. Le Lay, *Sci. Rep.*, 2013, 3.
14. C. Léandri, H. Oughaddou, B. Aufray, J. M. Gay, G. Le Lay, A. Ranguis and Y. Garreau, *Surf. Sci.*, 2007, 601, 262-267.
15. J. Gao and J. Zhao, *Sci. Rep.*, 2012, 2.
16. M. Houssa, G. Pourtois, V. V. Afanas'ev and A. Stesmans, *Appl. Phys. Lett.*, 2010, 96, -.
17. L. Li, S.-z. Lu, J. Pan, Z. Qin, Y.-q. Wang, Y. Wang, G.-y. Cao, S. Du and H.-J. Gao, *Adv. Mater.*, 2014, 26, 4820-4824.
18. N. D. Drummond, V. Zólyomi and V. I. Fal'ko, *Phys. Rev. B*, 2012, 85, 075423.
19. J. Liu and W. Zhang, *RSC Adv.*, 2013, 3, 21943-21948.
20. Z. Ni, Q. Liu, K. Tang, J. Zheng, J. Zhou, R. Qin, Z. Gao, D. Yu and J. Lu, *Nano Lett.*, 2011, 12, 113-118.

21. Y. Li and Z. Chen, *J. Phys. Chem. C*, 2013, 118, 1148-1154.
22. Y. Ding and Y. Wang, *J. Phys. Chem. C*, 2014, 118, 4509-4515.
23. J. E. Padilha, L. Seixas, R. B. Pontes, A. J. R. da Silva and A. Fazzio, *Phys. Rev. B*, 2013, 88, 201106.
24. R. Quhe, R. Fei, Q. Liu, J. Zheng, H. Li, C. Xu, Z. Ni, Y. Wang, D. Yu, Z. Gao and J. Lu, *Sci. Rep.*, 2012, 2.
25. R. Wang, X. Pi, Z. Ni, Y. Liu, S. Lin, M. Xu and D. Yang, *Sci. Rep.*, 2013, 3.
26. H. Liu, J. Gao and J. Zhao, *J. Phys. Chem. C*, 2013, 117, 10353-10359.
27. C.-w. Zhang and S.-s. Yan, *J. Phys. Chem. C*, 2012, 116, 4163-4166.
28. V. O. Özçelik, E. Durgun and S. Ciraci, *J. Phys. Chem. C*, 2014, 5, 2694-2699.
29. H. Şahin, S. Cahangirov, M. Topsakal, E. Bekaroglu, E. Akturk, R. T. Senger and S. Ciraci, *Phys. Rev. B*, 2009, 80, 155453.
30. E. Scalise, M. Houssa, G. Pourtois, B. Broek, V. Afanas'ev and A. Stesmans, *Nano Res.*, 2013, 6, 19-28.
31. J.-A. Yan, R. Stein, D. M. Schaefer, X.-Q. Wang and M. Y. Chou, *Phys. Rev. B*, 2013, 88, 121403.
32. Z. Li and J. P. Carbotte, *Phys. Rev. B*, 2013, 88, 045417.
33. J. N. Coleman, M. Lotya, A. O'Neill, S. D. Bergin, P. J. King, U. Khan, K. Young, A. Gaucher, S. De, R. J. Smith, I. V. Shvets, S. K. Arora, G. Stanton, H.-Y. Kim, K. Lee, G. T. Kim, G. S. Duesberg, T. Hallam, J. J. Boland, J. J. Wang, J. F. Donegan, J. C. Grunlan, G. Moriarty, A. Shmeliov, R. J. Nicholls, J. M. Perkins, E. M. Grieveson, K. Theuwissen, D. W. McComb, P. D. Nellist and V. Nicolosi, *Science*, 2011, 331, 568-571.
34. L. Rast, T. J. Sullivan and V. K. Tewary, *Phys. Rev. B*, 2013, 87, 045428.